JACS
JOURNAL OF THE AMERICAN CHEMICAL SOCIETY

Article

pubs.acs.org/JACS

Synthesis, Computed Stability, and Crystal Structure of a New Family of Inorganic Compounds: Carbonophosphates

Hailong Chen, Geoffroy Hautier,[§] and Gerbrand Ceder*

Department of Materials Science and Engineering, Massachusetts Institute of Technology, 77 Massachusetts Avenue, Cambridge, Massachusetts 02139, United States

Supporting Information

ABSTRACT: *Ab initio*-based high-throughput computing and screening are now being used to search and predict new functional materials and novel compounds. However, systematic experimental validation on the predictions remains highly challenging, yet desired. Careful comparison between computational predictions and experimental results is sparse in the literature. Here we report on a systematic experimental validation on previously presented computational predictions of a novel alkali carbonophosphate family of compounds. We report the successful hydrothermal synthesis and structural characterization of multiple sodium carbonophosphates. The experimental conditions for formation of the carbonophosphates and the computational results are compared and discussed. We also demonstrate topotactic chemical de-sodiation of one of the compounds, indicating the potential use of this novel class of compounds as Li^+ or Na^+ insertion electrodes.

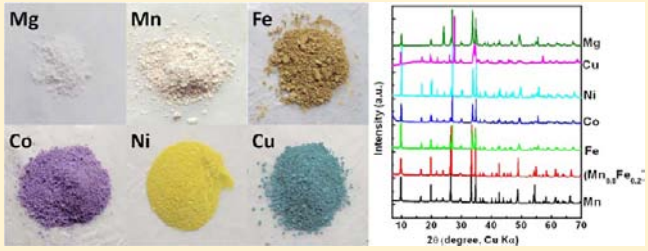

INTRODUCTION

Novel materials are the key to the development of new devices and technologies. Conventionally, the discovery of new compounds relies solely on experimental approaches, which require the testing of many synthesis conditions and parameters and can be very time consuming. *Ab initio* computation, whereby the properties and existence of new compounds are predicted, can bring some efficiency to this process. In particular, scaling these computational approaches so that thousands of possible compounds can be evaluated holds promise for the discovery of novel, interesting compounds. Recently, high-throughput computational searches have been performed to evaluate materials for Li-ion batteries,[1−3] scintillators,[4] and thermoelectrics.[5] This novel approach certainly expedites the process of exploring chemical spaces and can even lead to the prediction of entirely novel compounds based on computational thermodynamical analysis.[6−8] However, it remains difficult and challenging to actually synthesize the predicted new materials. The difficulty comes not only from the limited synthetic resources that any single research group can provide, but more particularly from the absence of relevant experimental literature to consult, especially when attempting to synthesize compounds of completely new or rarely explored chemical classes. In this paper, we investigate the synthesis of one such computationally predicted, and chemically unusual class of materials: the carbonophosphates.

In previous high-throughput computing work, we have reported the possible existence of new classes of mixed polyanionic compounds as potential Li-ion cathode materials.[9] Among the compounds with the general formula of $A_xM(YO_3)(XO_4)$ (A = Li, Na; Y = S, P, Si, As; X = C, B; M = redox-active metal; and x = 1−3), the sodium transition-metal carbonophosphates (A = Na; M = transition metals; Y = C; X = P; and x = 2 or 3) represent the most stable chemical class. While *ab initio* computations predict sodium carbonophosphates to be thermodynamically stable for many different transition metals, experimental results on carbonophosphates are extremely rare. Four carbonophosphates, with M = Mn, Fe, Sr, or Mg, were reported in the 1980s as rare natural minerals, but no reports on the artificial synthesis of these compounds exist. In this work, we report the successful laboratory synthesis of multiple carbonophosphates, including the above four minerals, as well as other new members of this class, and discuss their formation conditions. The crystal structure of each compound is characterized by synchrotron powder X-ray diffraction (XRD) and Rietveld refinement. We further show that these carbonophosphates can be chemically de-sodiatied, implying that this new class of compounds may be able to undergo reversible Na-ion intercalation/de-intercalation reactions and function as Na-ion electrode materials. Na-ion batteries represent a promising rechargeable battery technology that would share many operating mechanisms with Li-ion batteries.[10−14]

METHODS

1. Computation Methods. All *ab initio* computations have been performed with the VASP software suite[15] within the density functional theory (DFT) framework using the generalized gradient approximation from Perdew, Burke, and Ernzerhof (GGA-PBE)[16] and a Hubbard U parameter for some transition metals.[17] More details on

Received: May 2, 2012
Published: October 19, 2012

dx.doi.org/10.1021/ja3040834 | J. Am. Chem. Soc. 2012, 134, 19619−19627

the specific parameters can be found in the works of Jain et al.[2] and Hautier et al.[9]

Thermodynamic stability was evaluated by using the convex hull construction which compares the structure's energy to linear combinations of the energy of other phases that result in the same overall composition. Figure 1a illustrates the convex hull construction

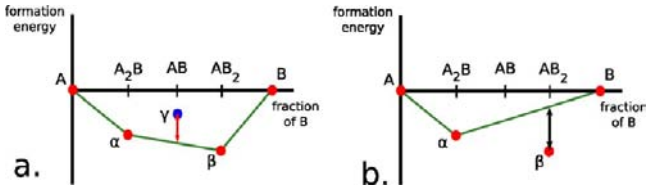

Figure 1. Construction of the convex hull of a hypothetical A-B system, where A and B are different elements. α, β, and γ are the hypothetical phases with compositions of A_2B, AB_2, and AB, respectively. The *energy above the hull* and *energy below the hull* are indicated by the red (a) and black (b) arrows, respectively.

on a simple example of an A-B system. The x axis indicates the fraction of B and the y axis the energy of the phase. Three binary phases are present: α, β, and γ. The convex hull drawn in green indicates that the α and β phases are stable while the γ phase is unstable versus decomposition in α and β. The stability analysis of any new compound was performed versus all compounds present in the Inorganic Crystal Structure Database (ICSD)[18a] plus a set of phosphates predicted in our previous work.[2] The energy of the O_2 molecule used is obtained from Wang et al.,[19] and the CO_2 energy is fitted as in Hautier et al.[9] We neglected the entropy component of solid phases. The entropy values of O_2 and CO_2 gases were obtained from the experimental JANAF tables.[20] We set the partial pressure of O_2 and CO_2 to their values in air ($p_{O_2} = 0.21$, $p_{CO_2} = 10^{-4}$) and the temperature to 298 K (25 °C).

We quantify a compound's thermodynamic instability by computing the *energy above the hull*, which represents the compound's energy for decomposition to stable products. An *energy above the hull* is always positive and measures the thermodynamic driving force for the compound to decompose into a set of alternate phases. A thermodynamically stable compound will have an *energy above the hull* of 0 eV/atom, as it is part of the convex hull of stable phases. The *energy above the hull* of phase γ in a simple hypothetical A-B system is presented in Figure 1a by the red arrow.

We evaluated the stability of a stable phase by computing the *energy below the hull*, which is the negative energy of formation of the phase of interest from the phases that would be stable if the compound did not exist. It is a positive number and expressed in eV/atom. A large *energy below the hull* represents a high stability of the stable compound. The *energy below the hull* of phase β in a simple hypothetical A-B system is presented in Figure 1b by the black arrow.

The equilibrium simplex that contains the composition of an unstable phase in the computed phase diagram is also of interest, as it indicates which more stable phases prevent the compound from being stable. In Figure 1a, the γ phase lies in the equilibrium simplex composed of α and β. An equilibrium simplex can also be defined for stable phases by the phases that would be the equilibrium simplex for the compound if it was not stable. In Figure 1b, the equilibrium simplex for β is α and the elemental B phase.

2. Synthesis. We attempted the syntheses of most of the carbonophosphate compounds that were computationally identified to be stable, except for a few compounds that contain highly toxic elements, e.g., the Cd and Tl versions. A typical synthesis route is described below using the Mn version as an example. First, 0.002 mol of $Mn(NO_3)_2{\cdot}4H_2O$ is dissolved in 5 mL of water to form a clear solution (A). Separately, 0.002 mol of $(NH_4)_2HPO_4$ and 2 g of Na_2CO_3 are dissolved in 10 mL of water to form a clear solution (B). Solution (A) is then quickly added to solution (B) under fast magnetic stirring. The mixture slurry is then transferred to an autoclave with a poly(tetrafluoroethylene) liner and sealed with caps. The autoclave is heated in an oven or oil bath at 160 °C for 20 h. After the autoclave is slowly cooled to room temperature, the products are washed with distilled water and methanol several times, followed by drying in a vacuum oven at 40 °C overnight. To obtain a phase-pure sample, the synthesis temperature of the Mn compound can be varied from 90 to 240 °C, with the heating time adjusted accordingly. At 90 °C, a single-phase product is obtained after 8 h with magnetic stirring or after 24–48 h without stirring. At 120 °C and above, 2 h reaction time is enough to form a single-phase sample with stirring applied. To ensure good enough crystallinity for structure characterization, commonly 20 h reaction time is used. The Mn sample used for XRD measurement was synthesized at 120 °C for 20 h and with magnetic stirring.

To synthesize other carbonophosphates, the metal source in the starting materials is changed according to the desired compound, while $(NH_4)_2HPO_4$ and Na_2CO_3 are kept as the phosphorus and carbon sources. $Sc(NO_3)_3{\cdot}H_2O$, VCl_2 (and VCl_3), $Cr(NO_3)_3{\cdot}9H_2O$, $FeSO_4{\cdot}7H_2O$, $Co(NO_3)_2{\cdot}6H_2O$, $Ni(NO_3)_2{\cdot}6H_2O$, $CuCl_2$, $Zn(NO_3)_2{\cdot}6H_2O$, $Mg(NO_3)_2{\cdot}6H_2O$, $Ca(NO_3)_2{\cdot}4H_2O$, $Sr(NO_3)_2$, $Ba(NO_3)_2$, $Y(NO_3)_3{\cdot}6H_2O$, $MoCl_3{\cdot}6H_2O$, $Al(NO_3)_2{\cdot}9H_2O$, and $Bi(NO_3)_2{\cdot}5H_2O$ are used for the syntheses of the Sc, V, Cr, Fe, Co, Ni, Cu, Zn, Mg, Ca, Sr, Ba, Y, Mo, Al, and Bi versions. To obtain the desired phase, the concentration of the starting materials, temperature (up to 240 °C), and reaction time are varied in each case.

3. Characterization. All the powder samples were characterized by XRD. Mg and Cu samples data were collected using a Rigaku miniflex II diffractometer (chromium Kα, λ = 2.2897 Å) with flat-plate mode, scanning from 10 to 120° two-theta. Mn, Fe, Co, and Ni sample data were collected using synchrotron radiation at beamlines X14A (λ = 0.7752 Å) and X16C (λ = 0.6993 Å) at the National Synchrotron Light Source at Brookhaven National Laboratory (NSLS-BNL). The data were collected in transmission mode by using 1.0 or 1.5 mm glass capillaries, scanning from 4 to 45° two-theta. The capillaries were spun ~120 rpm. The data were collected with a silicon strip detector, and typically 20–40 min was needed for each sample. For clarity, all two-theta values in the XRD data are converted to the two-theta value of Cu Kα wavelength when shown in figures below. The scanning electron microscope (SEM) images were taken using a JEOL 6032 SEM. Refinements of the XRD patterns were performed using a GSAS code.

4. Chemical De-sodiation. Chemical de-sodiation was performed for the $Na_3Fe(CO_3)(PO_4)$ sample. In a typical procedure, 100 mg of the sodium iron carbonophosphate powder was added into 50 mL of 0.5 M $K_2S_2O_8$ solution, followed by stirring at 600 rpm for 3 h. The product was separated from the solution by centrifugation and washed several times with distilled water and methanol. The wet paste was then dried in a vacuum oven at 50 °C overnight, followed by structural examination with XRD.

■ RESULTS

Figure 2 shows the structure of the natural mineral sidorenkite.[21] We refer to this structure as the sidorenkite structure hereafter. In this structure, the tetrahedral PO_4 groups and the MO_6 octahedra corner-share to form double layers as the basic framework. The triangular planar CO_3 groups sit on the side of the double layers, sharing two O atoms with the MO_6 octahedra. The Na atoms occupy the interstitial sites between the double layers. There are two different Na sites in the unit cell, coordinated with six (multiplicity = 4, shown as Na1 in Figure 2) and seven (multiplicity = 2, shown as Na2 in Figure 2) oxygen atoms, respectively.

In previous work[9] we reported the computed stability of this structure with the general formula $A_xM(YO_3)(XO_4)$ (A = Li, Na; Y = S, P, Si, As; X = C, B; M = redox-active metal; and x = 1–3). Only redox-active metals in the M site were evaluated in ref 9, as these compounds are being considered as potential electrode materials for Li-ion or Na-ion batteries, where the

dx.doi.org/10.1021/ja3040834 | J. Am. Chem. Soc. 2012, 134, 19619–19627

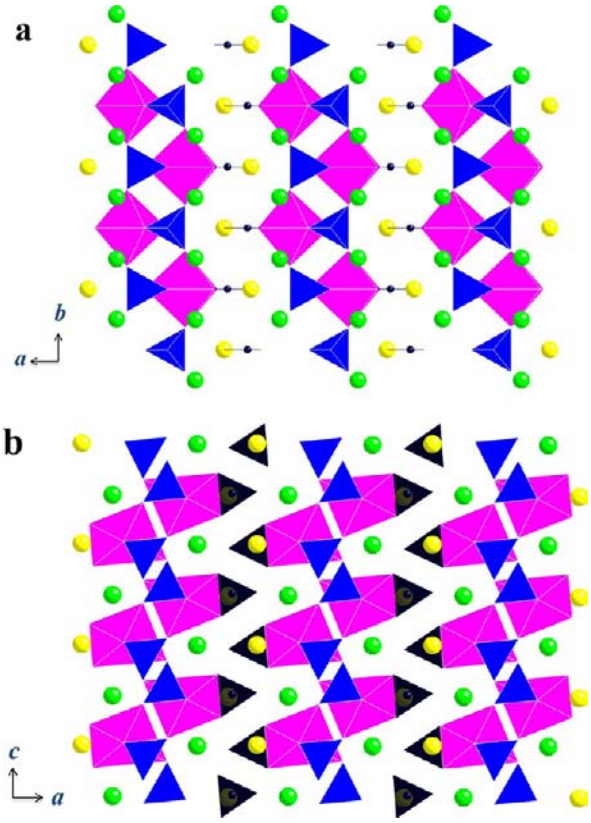

Figure 2. Structure of $Na_3MPO_4CO_3$ (M = Mn, Fe, etc.) viewed from [001] (a) and [010] (b). Transition metal octahedra, purple; PO_4 tetrahedra, blue; CO_3 triangle planar, black; Na, green (Na1) and yellow balls (Na2).

metal in the M site must be able to change oxidation states to compensate for electrochemical Na^+ or Li^+ extraction. In this work, to explore the general thermodynamic stability of this chemical class in a wider range of chemistry, many non-redox-active metals, such as the alkaline earth metals, have also been considered.

Tables 1 and 2 show the stability of the carbonophosphate compositions that have been computed. Table 1 refers to compounds with M^{2+} ions ($Na_3M(CO_3)(PO_4)$ compositions) and Table 2 to compounds with M^{3+} ions ($Na_2M(CO_3)(PO_4)$ compositions). The *energy above the hull* is the computed energy of decomposition to stable compounds in our phase diagram in eV/atom (see Methods section for more details). An *energy above the hull* of zero indicates a stable compound in the conditions we considered. The larger the energy above the hull, the less stable is the compound. The *energy below the hull* is the negative of the energy of formation of the phase of interest from the phases that would be stable if it did not exist for the most competitive equilibrium (see Methods section). The larger the *energy below the hull*, the more stable is the stable phase. We also indicated the equilibrium simplex, which shows in which part of the phase diagram the phase lies and what the directly competing phases are (see Methods section).

In total, 16 carbonophosphates with the sidorenkite structure are predicted to be stable, including both 2+ (Mg^{2+}, Ni^{2+}, Fe^{2+}, Mn^{2+}, Cd^{2+}, Ca^{2+}, Co^{2+}, Cu^{2+}, and Zn^{2+}) and 3+ (Fe^{3+}, V^{3+}, Cr^{3+}, Bi^{3+}, Mo^{3+}, Sc^{3+}, and Al^{3+}) metals. As mentioned by Hautier et al.,[9] all the M^{3+}-containing phases are in an equilibrium simplex involving CO_2, and their stability therefore depends directly on the chemical potential of CO_2, which varies with synthesis conditions (e.g., temperature). All our analysis was based on using a μ_{CO_2} representing air at 25 °C (see Methods section). A higher temperature, for instance, would decrease the μ_{CO_2} and may destabilize the 3+ metal compounds. On the other hand, none of the stable 2+ metal compounds are found to be in equilibrium with CO_2 gas.

Syntheses were attempted for most of the carbonophosphate compounds that are computationally identified to be stable, and a few that are slightly nonstable, except for the Cd and Tl compounds. Thermal stability tests on the natural minerals indicate that the natural sidorenkite mineral decomposes at ~650 °C and releases CO_2. This implies that a simple solid-state reaction method, which usually requires a reaction temperature higher than 700 °C to decompose the starting materials, might not be appropriate for the synthesis of the carbonophosphates. Wet chemistry methods (e.g., hydro-

Table 1. Computed Stability and Experimental Results on Carbonophosphate Compounds $Na_3MCO_3PO_4$, with M = 2+ Valence Metals

metal at M^{2+} site	E. above hull (eV/atom)	E. below hull (eV/atom)	equilibrium simplex	typical synthesis conditions (temp, time)	synthesis results
Mg	on the hull	0.029	Na_2CO_3, $NaMgPO_4$	220 °C, 20 h	$Na_3MgCO_3PO_4$
Ni	on the hull	0.025	Na_2CO_3, $NaNiPO_4$	220 °C, 20 h	$Na_3NiCO_3PO_4$
Fe	on the hull	0.023	Na_2CO_3, $NaFePO_4$	120 °C, 20 h	$Na_3FeCO_3PO_4$
Mn	on the hull	0.019	Na_2CO_3, $NaMnPO_4$	120 °C, 20 h	$Na_3MnCO_3PO_4$
Cd	on the hull	0.015	Na_2CO_3, $NaCdPO_4$	N/A	not attempted
Ca	on the hull	0.013	Na_3PO_4, $NaCaPO_4$, $Na_2Ca_2(CO_3)_3$	220 °C, 20 h	$Ca_3(PO_4)_2{\cdot}xH_2O$ and $Ca_8H_2(PO_4)_6$–$NaHCO_3$–H_2O
Co	on the hull	0.008	Na_2CO_3, $NaCoPO_4$	120 °C, 20 h	$Na_3CoCO_3PO_4$
Cu	on the hull	0.006	$Na_4P_2O_7$, CuO, $Na_2Cu(CO_3)_2$	220 °C, 20 h	$Na_3CuCO_3PO_4$
Zn	on the hull	0.002	Na_2CO_3, $NaZnPO_4$	240 °C, 20 h	unidentified solid phase(s)
Cr	0.007	N/A	Na_2CO_3, Cr_2O_3, $Na_4P_2O_7$, C, CO_2[a]	240 °C, 20 h	amorphous phase
Sr	0.01	N/A	Na_3PO_4, $SrCO_3$	240 °C, 20 h	$Na_3SrCO_3PO_4$ and $SrCO_3$
V	0.012	N/A	$Na_4P_2O_7$, $Na_3V_2(PO_4)_3$, V_2O_3, C, Na_2CO_3,	240 °C, 20 h	amorphous phase
Ba	0.05	N/A	Na_3PO_4, $BaCO_3$	240 °C, 20 h	$BaCO_3$

[a]The simplex containing CO_2.

dx.doi.org/10.1021/ja3040834 | J. Am. Chem. Soc. 2012, 134, 19619–19627

Table 2. Computed Stability and Experimental Results on Carbonophosphate Compounds $Na_2MCO_3PO_4$ with M = 3+ Valence Metals

metal at M^{3+} site	E. above hull (eV/atom)	E. below hull (eV/atom)	equilibrium simplex	typical synthesis conditions (temp, time	synthesis results
Fe	on the hull	0.008	$Na_4P_2O_7$, Fe_2O_3, CO_2[a]	180 °C, 20 h	amorphous phase
V	on the hull	0.008	Na_2CO_3, Sc_2O_3, $Na_3V_2(PO_4)_3$, CO_2[a]	180 °C, 20 h	amorphous phase
Cr	on the hull	0.006	$Na_4P_2O_7$, V_2O_3, CO_2[a]	180 °C, 20 h	amorphous phase
Bi	on the hull	0.005	Na_2CO_3, $BiCO_5$, $Na_3Bi(PO_4)_2$, CO_2[a]	220 °C, 20 h	$BiOCO_3$
Mo	on the hull	0.001	$Na_4P_2O_7$, MoO_2, C, CO_2[a]	220 °C, 20 h	amorphous phase
Sc	on the hull	0	Na_2CO_3, Sc_2O_3, $Na_3Sc_2(PO_4)_3$, CO_2[a]	220 °C, 20 h	unidentified solid phase(s)
Al	on the hull	0	$Na_4P_2O_7$, Al_2O_3, CO_2[a]	240 °C, 20 h	unidentified solid phase(s)
Mn	0.001	N/A	$Na_4P_2O_7$, Mn_2O_3, CO_2[a]	180 °C, 20 h	not attempted
In	0.004	N/A	Na_2CO_3, In_2O_3, $Na_3In(PO_4)_2$, CO_2[a]	220 °C, 20 h	InOOH
Ga	0.007	N/A	$Na_4P_2O_7$, Ga_2O_3	N/A	not attempted
Sb	0.011	N/A	$Na_4P_2O_7$, Sb_2O_3, CO_2[a]	N/A	not attempted
Tl	0.013	N/A	$Na_4P_2O_7$,Tl_2O_3, CO_2[a]	N/A	not attempted
Y	0.024	N/A	Na_3PO_4, YPO_4, $Na_5Y(CO_3)_4$	220 °C, 20 h	unidentified solid phase(s)
Co	0.029	N/A	$Na_4P_2O_7$, Co_3O_4, O_2, CO_2[a]	N/A	not attempted
Cu	0.032	N/A	$Na_4P_2O_7$, CuO, O_2, CO_2[a]	N/A	not attempted

[a]The simplex containing CO_2.

thermal) are alternative routes to synthesize these compounds. Hydrothermal methods have been extensively used to synthesize phosphates,[22] carbonates,[23] or mixed polyanion compounds such as fluorophosphates.[24] Many metal carbonates and phosphates are not soluble in aqueous solutions. Therefore, it is presumably possible to obtain carbonophosphate precipitates by mixing water-soluble starting materials. After trying various starting materials and reaction conditions, the first carbonophosphate phase, i.e., the Mn phase, was observed as a minor phase in a mixed hydrothermal reaction product. After further optimization of the synthesis conditions such as the ratio and concentration of starting materials and reaction temperature, phase-pure $Na_3Mn(PO_4)(CO_3)$ was obtained. We found that the molar ratio of the carbonates and phosphates in the hydrothermal solution is a key factor to form phase-pure carbonophosphates. Defining $R = [CO_3^{2-}]/([PO_4^{3-}] + [CO_3^{2-}])$, for the case of manganese carbonophosphate synthesis, $R > 7/8$ is required to obtain phase-pure samples at any temperature. A smaller R value leads to the presence of competing phases. For example, when $R = 3/4$, approximately 1:1 (wt%) mixed $Na_3Mn(PO_4)(CO_3)$ and $MnCO_3$ phases resulted; when $R = 1/2$, only $NaMnPO_4$ and $MnCO_3$ phases were formed. When R is fixed at 7/8, $Na_3Mn(PO_4)(CO_3)$ can be formed in a rather wide range of temperature (i.e., 90−240 °C). We did not test temperatures above 240 °C because the safety limit of the Parr 4749 autoclaves is 250 °C. Due to the fairly high viscosity of the slurry-like hydrothermal solution, the reaction time is greatly affected by the exchange rate between the solution and the precursor/intermediate phases. With 600 rpm magnetic stirring, the reaction commonly finishes within 12 h at 90 °C, compared to 2−3 days without stirring. Meanwhile, strong stirring could create more nucleation sites, which would also shorten the reaction time. Reaction time is also affected by temperature. At 120 °C, a phase-pure sample can be obtained after only 2 h under stirring.

Following similar procedures, several other carbonophosphates were successfully synthesized, and the results are summarized in Table 1. In summary, seven carbonophosphates (Fe, Co, Mn, Ni, Cu, Mg, and Sr) are obtained, though the Sr sample was not single phase (mixed with $SrCO_3$ and an unidentified minor phase), and the Cu version contains a very minor unidentified impurity phase. The Co, Ni, and Cu phases are completely new compounds. The Fe, Mn, Mg, and Sr phases are synthesized in the laboratory for the first time. It is worth noting that $Na_3SrPO_4CO_3$, although having a formula similar to that of the other sidorenkites, has been reported to have a different crystal structure: crawfordite.[18a] The crawfordite and sidorenkite structures are only slightly different. The XRD pattern of our sample can match the simulated patterns using both structures by varying the cell parameters a bit. However, the XRD pattern simulated using both structures does not match the pattern in the Powder Diffraction File (PDF)[18b] database, which indicates a rare inconsistency between ICSD and PDF databases. The computational results indicate that the energy of the strontium carbonophosphate in the sidorenkite structure is 5 meV/atom lower than in the crawfordite structure. With our current sample being a mixture of three phases and our inability to produce a single-phase sample, it is difficult to conclusively determine the structure of the strontium carbonophosphate. The attempts to synthesize the V, Cr, Ca, Ba, Sc, Y, Mo, Al, Zn, and Bi versions failed, even with the most extreme conditions that we can currently reach, such as high temperature and high/low concentrations. We also noticed that many solid solution phases can be made by mixing various transition metal sources in the starting materials. For example, a series of Fe−Mn solid solution phases, such as $Na_3(Fe_xMn_{1-x})(PO_4)(CO_3)$ (x = 0.1, 0.2, and 0.3)[25] and $Na_3(Co_{0.5}Mn_{0.5})(PO_4)(CO_3)$ (see Figure S2 in Supporting Information for XRD pattern), have also been synthesized which implies that, at least for Fe, Mn, and Co, it is very possible to obtain 0−100% solid solution in the sidorenkite structure with any two or more of these elements.

The carbonophosphate compounds show different colors depending on the different metal element in the M site. As

dx.doi.org/10.1021/ja3040834 | J. Am. Chem. Soc. 2012, 134, 19619−19627

Figure 3. The colors of different $Na_3MPO_4CO_3$ carbonophospahtes: M = Mg (a), Mn (b), Fe (c), Co (d), Ni (e), and Cu (f).

shown in Figure 3, the Ni, Cu, and Co samples are bright yellow, dark green, and magenta, respectively. Both Sr (not shown in Figure 3) and Mg samples are pure white. The Mn sample is light beige. It is also worth noting that, because of the fast oxidation of Fe(II) compounds to Fe(III) in air, synthesis of the pure or mixed iron carbonophosphates was carried out in an Ar-flushed glovebox. However, during the washing procedure, it is still possible for some of the surface Fe(II) to become oxidized to Fe(III) upon the short exposure to air or to the dissolved O_2 in distilled water and methanol. The oxidation of Fe(II) was evidenced by a color change of the powder from very light green to light brownish (Figure 3c) after the washing and drying process.

The presence of the sidorenkite unit cell was confirmed with XRD for all the synthesized samples. Figure 4 shows the XRD

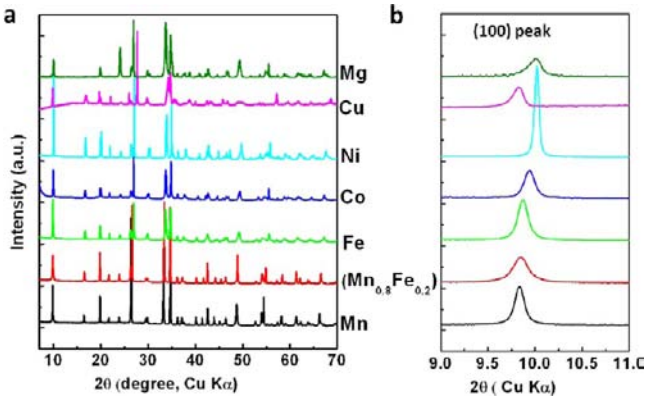

Figure 4. (a) XRD patterns of $Na_3MPO_4CO_3$ carbonophosphates: M = Mn, $Mn_{0.8}Fe_{0.2}$, Fe, Co, Ni, Cu, and Mg. (b) Enlarged 9−11° region.

patterns of the Mg, Mn, Fe, Co, Ni, and Cu carbonophosphates and an example of the mixed version, $Na_3(Fe_{0.2}Mn_{0.8})(PO_4)(CO_3)$. The XRD pattern of the Sr version is shown in Figure S1 in the Supporting Information. The XRD patterns of these compounds (Figure 4) are similar to each other and can be indexed with the reported sidorenkite mineral structure, suggesting they are isostructural. There are slight differences in the peak positions of the different compounds, due to the cell parameter change with the differences in transition metal ion size. Such shifts in peak positions can be better viewed in the inset of Figure 4, which shows a zoomed-in view of the (100) reflections.

Rietveld refinements were performed for high-resolution synchrotron XRD patterns of the Fe, Mn, Co, and Ni samples, using the mineral sidorenkite as a structure model (space group $P2_1/m$). Figure 5 shows the refinements on the Ni and Co samples, synthesized at 180 °C, 20 h and 120 °C, 20 h, respectively. Refinements for Mg and Cu samples were performed with data collected on laboratory X-ray diffractometers with overnight scans. The refinements of all the samples are shown in Figure S4 in the Supporting Information. Good fits were obtained for all the samples, which confirmed the structural model of carbonophosphates extracted from the natural minerals by Khomyakov et al.[21] The cell parameters of the carbonophosphates are summarized in Table 3. CIF files for the Fe, Mn, Co, Ni, Mg, and Cu compounds are included in the Supporting Information.

The chemical compositions (Table S1 in Supporting Information) of some of the synthesized carbonophosphate compounds were obtained by inductively coupled plasma atomic emission spectrometry. The Sr and Cu versions were not analyzed due to the presence of impurity phases. The Mn sample synthesized at 120 °C, 3 d shows a composition very close to stoichiometry. The Co sample, from which the XRD pattern was collected, was synthesized at 120 °C, 20 h. It shows an excess amount of Co (Table S1) and a high background, and an identified impurity peak (indicated by the arrow in Figure 5a) in the XRD pattern. To test whether the formation reaction of the Co sidorenkite did not complete at 120 °C, we repeated the synthesis at higher temperature, 220 °C. The high-temperature sample shows a composition very close to stoichiometry. Similarly, the Ni sample synthesized at higher temperature (220 °C) is more stoichiometric than the sample synthesized at lower temperature (180 °C). Hence, it seems likely that the lower temperature syntheses for the Co and Ni contain amorphous products that modify the overall stoichiometry of the sample. The Fe sample also shows a slight excess of Fe, but for this compound increasing synthesis temperature does not eliminate/reduce the off-stoichiometry.

dx.doi.org/10.1021/ja3040834 | J. Am. Chem. Soc. 2012, 134, 19619−19627

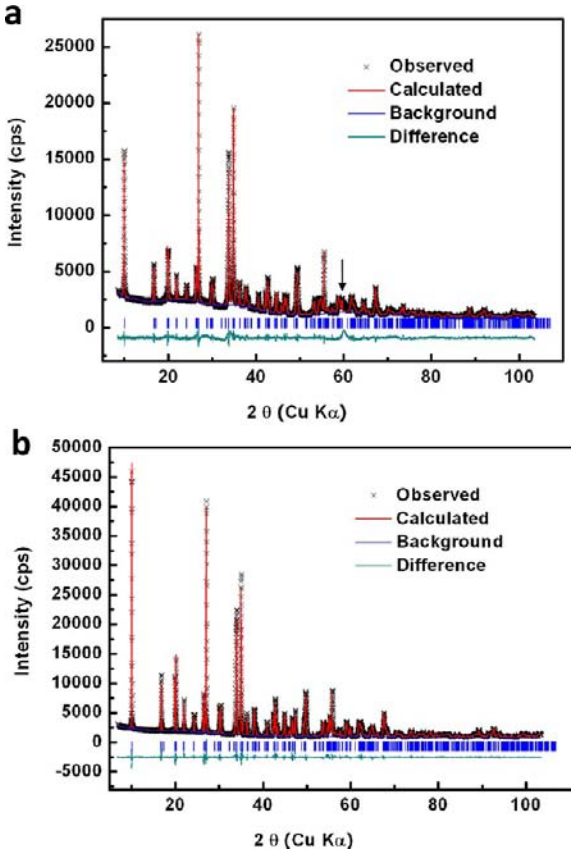

Figure 5. XRD patterns and refinements of (a) $Na_3CoPO_4CO_3$ and (b) $Na_3NiPO_4CO_3$. The black arrow in (a) indicates the peak of an unidentified impurity phase.

We believe that the off-stoichiometry arises from oxidation of Fe(II) to Fe(III) upon exposure to air/water during the synthesis, washing, and drying procedure with formation of some amorphous phase on the surface.[26] To obtain very stoichiometric iron carbonophosphate, the use of nonaqueous solvent and washing/drying under inert atmosphere are required.

The particle morphology of the carbonophosphates was examined using scanning electron microscopy (SEM). Figure 6a,b shows the SEM images of the Fe samples synthesized with and without magnetic stirring. This is a good example demonstrating how stirring can significantly affect crystal growth and morphology during the hydrothermal synthesis. When stirring is applied, fine particles with plate-like morphology and ~300−500 nm size are formed. Without stirring, particles grow in an interesting walnut-like morphology. These secondary self-assembled particles are a few micrometers in size and are formed from plate-like primary particles. The Ni sample obtained without stirring shows a morphology similar to that of the Fe sample but with larger particle sizes in both primary and secondary particles. Interestingly, for the Co and Mn samples, no such self-assembled secondary particles are seen. Figure 6c,d shows the SEM images of the Co samples without and with stirring, respectively. The sample with stirring shows slightly smaller particle size, likely because stirring created more nucleation sites during the reaction.

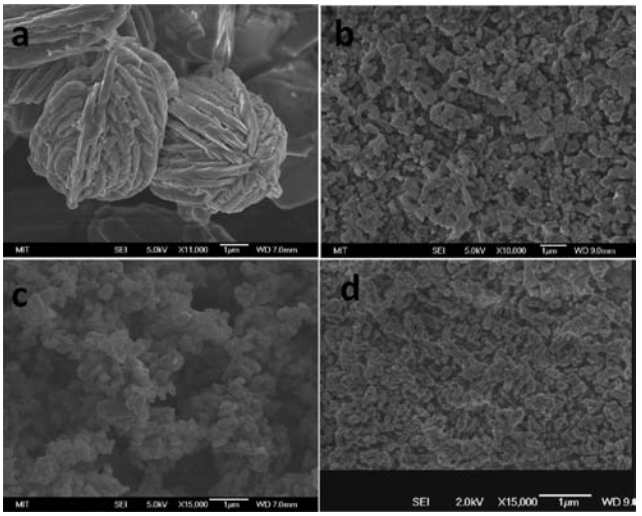

Figure 6. SEM images of the carbonophosphates: (a) Fe sample without stirring, (b) Fe sample with stirring, (c) Co sample without stirring, and (d) Co sample with stirring. The scale bars are 1 μm.

In our previous work, the lithium carbonophosphates were predicted and experimentally[26] demonstrated to be able to topotactically intercalate and de-intercalate lithium in Li-ion battery cells. The current renewed interest in Na-based batteries[12,13] motivates the study of Na de-intercalation in the sidorenkite compounds. To test the possibility of topotactic de-intercalation of Na, we proceeded with chemical de-sodiation. Figure 7 shows the XRD patterns of sodium iron carbonophosphate samples before (pristine) and after (de-sodiated) 3 h treatment with 0.5 M $K_2S_2O_8$ solution. The positions of the XRD reflections of the de-sodiated sample are very similar to those of pristine sample but with slight shifts, suggesting that

Table 3. Cell Parameters Extracted from XRD Refinement of the Carbonophosphates

metal	a (Å)	b (Å)	c (Å)	β (deg)	V (Å)	r (Å)	χ^2	R_{wp} (%)	R_p (%)
Mg	8.83	6.62	5.16	89.69	301.1	0.72	3.48	5.81	4.31
Mn	8.99	6.74	5.16	90.12	312.3	0.83 (hs) 0.67 (ls)	5.78	6.5	4.76
Fe	8.95	6.61	5.16	89.60	305.4	0.78(hs) 0.61 (ls)	3.33	4.33	3.23
Co	8.89	6.62	5.15	89.49	302.8	0.75 (hs) 0.65 (ls)	6.45	5.74	4.14
Ni	8.83	6.59	5.13	89.27	298.1	0.69	5.37	5.36	3.94
Cu	9.01	6.44	5.17	88.94	299.5	0.73	4.3	3.4	2.4
Sr[a]	9.18	6.71	5.28	89.16	324.9	1.18			

[a]The Sr data are from natural mineral.[18a]

dx.doi.org/10.1021/ja3040834 | J. Am. Chem. Soc. 2012, 134, 19619−19627

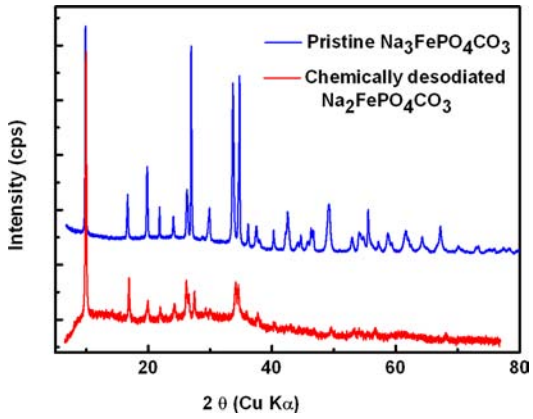

Figure 7. XRD patterns of sodium iron carbonophosphate before (blue) and after (red) chemical de-sodiation.

the lattice framework and symmetry are preserved after the treatment. However, the relative peak intensities of the de-sodiated sample differ significantly from those of pristine sample, which implies significant changes in site occupancy of the unit cell. Rietveld refinement was applied to the de-sodiated sample using the sidorenkite structure model (see Figure S4). The refinement results indicate that, after chemical de-sodiation, the cell parameters decrease from a = 8.95 Å, b = 6.61 Å, and c = 5.16 Å to a = 8.92 Å, b = 6.50 Å, and c = 5.19 Å. More importantly, refinement of the site occupancy shows that 94.5% of the seven-coordinated Na atoms (Na2 site in Figure 2) were extracted by reacting with $K_2S_2O_8$, while the six-coordinated Na atoms (Na1 site in Figure 2) remained intact. This result indicates that approximately one Na per formula is extracted from the structure. A similar chemical de-sodiation treatment was also applied for the Mn samples, but we did not observe any obvious changes in the XRD patterns before and after the treatment, plausibly due to the fact that Mn(II) is more difficult to oxidize by $K_2S_2O_8$ than Fe(II).

DISCUSSION

While a very large amount of phosphate and carbonate compounds have been reported, carbonophosphates constitute a much less studied chemical class but one that can be of technological interest (e.g., as insertion cathodes). In this work, we reported on the detailed hydrothermal synthesis, crystal structure, and computed stability of a series of carbonophosphates with formula $Na_xM(CO_3)(PO_4)$. We also demonstrated the possibility to de-intercalate Na topotactically through a chemical process.

It is still rare to demonstrate the synthesis of new compounds proposed by a computational analysis of thermodynamical stability, and this work gives the opportunity to assess the quality of those predictions as well as identify the limitations of this approach. Before comparing the computational predictions to the experimental results, a few caveats should be highlighted. DFT relies on approximations and possesses an inherent error in the energy it provides.[27] In addition, for the sake of computational cost, we neglected the entropic contribution to all solid phases, and only O_2 and CO_2 gases were assigned an entropic contribution. Moreover, our computational analysis consisted of studying the phase stability of the $Na_xM(CO_3)(PO_4)$ compounds vs solid and gaseous phases in a Na-M-C-P-O phase diagram at 298 K, but hydrothermal synthesis involves an aqueous environment and aqueous species in addition to solids and gases. Our approach defines, however, a necessary condition for synthesizability, as a phase unstable in the Na-M-C-P-O diagram will not be stable if additional aqueous species and water are added. We should note that current developments in the *ab initio* computations of Pourbaix phase diagrams will certainly alleviate this problem in the future and open up the possibility for assessing phase stability in conditions closer to hydrothermal synthesis.[28]

From the eight 2+-based compounds predicted to be stable and attempted (i.e., Fe, Ni, Co, Mn, Mg, Ca, Cu, Zn), we successfully synthesized six compounds (i.e., Fe, Ni, Co, Mn, Mg, Cu), showing a good success rate for the computational stability analysis in predicting the existence of new phases. All of the compounds we reported had never been synthesized before in a laboratory, and the Ni, Co, and Cu systems have never been reported as compounds. One of the unsuccessful syntheses was for the Zn compound, which is predicted to be only very mildly stable (*energy below the hull* of 2 meV/atom). The driving force for this compound to form may be too small to occur in hydrothermal synthesis, where the dissolution energy of the precursors has to be overcome (see below). The failure to synthesize the $Na_3Ca(PO_4)(CO_3)$ is more surprising given that it is predicted to be well below the convex hull of competing phases. However, the synthesis products identified by XRD after the hydrothermal process are all hydrated phases: $Ca_3(PO_4)_2{\cdot}xH_2O$ and $Ca_8H_2(PO_4)_6{-}NaHCO_3{-}H_2O$. Hence, The discrepancy between computations and experiments may be due to the fact that the hydrated phases were not computed in our stability analysis. They do not have an assigned crystal structure in the ICSD. Finally, we should note that the computational prediction indicating that the Ba phase would not be stable in the sidorenkite structure is consistent with our unsuccessful attempts in synthesizing $Na_3Ba(CO_3)(PO_4)$.

The experimental results are not as good for the M^{3+} compounds, none of which could be synthesized. There are several possible explanations for this. Hydrothermal synthesis works when (1) the reactants are soluble but the product phases are not, or (2) the product phases are more insoluble than the reactants, e.g., the solubility product constant K_{sp} of the product is smaller than that of the reactants. If the computed equilibrium simplex contains soluble phases, such as Na_2CO_3, then a large enough formation energy for the product phase is required, or else it would dissolve. For example, if the formation energy is zero, the product and reactants have the same energy, and since the reactants dissolve, so will the products. Hence, sufficiently large formation energy is required for successful hydrothermal synthesis. This is further evidenced by the failure for the $Na_3Zn(CO_3)(PO_4)$ to form among the M^{2+} compounds. The Zn compound has a very small formation energy. A further complication arises from the fact that all the 3+ compounds are in equilibrium with CO_2 (see Table 2). Any increase in temperature will favor the CO_2 phase (due to its higher entropy) by increasing the CO_2 chemical potential and thereby destabilize the $Na_2M(CO_3)(PO_4)$ (M = 3+ metal) phase. In the hydrothermal conditions, this μ_{CO_2} chemical potential can be related to the $(CO_3)^{2-}$ concentration. Hence, the difficulty to synthesize any 3+ compound might be linked to the limits of $(CO_3)^{2-}$ concentration that can be reached in the aqueous solution. The fact that a high ratio of $[CO_3^{2-}]/[PO_4^{3-}]$ is required in solution to synthesize the M^{2+} compounds further indicates that a high μ_{CO_2} may be required to achieve these phases.

dx.doi.org/10.1021/ja3040834 | J. Am. Chem. Soc. 2012, 134, 19619−19627

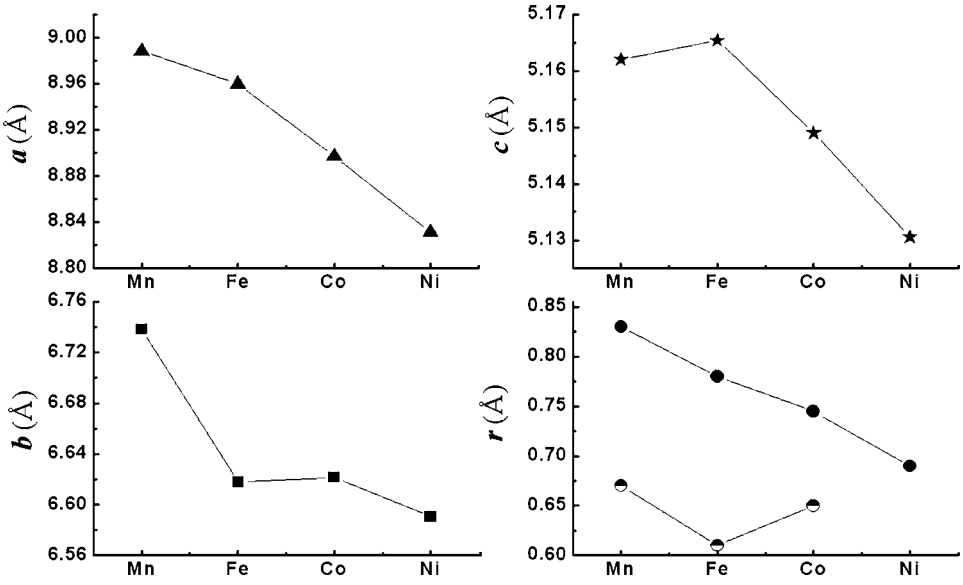

Figure 8. Cell parameters (*a*, *b*, and *c*) of carbonophosphates with the first-period transition metals and the Shannon ionic radii (*r*) of these transition metals with octahedral coordination (where filled circles indicate the radii of high-spin states, and half-filled circles indicate the radii of low-spin states).

Other than the sodium carbonophosphates, our stability computation[9] indicates that the Li versions of the carbonophosphate are not thermodynamically stable, though usually only by a slight amount. A few of them, such as $Li_3FePO_4CO_3$ and $Li_3MnPO_4CO_3$, can be obtained through Li−Na ion exchange from the sodium carbonophosphate precursors.[29] The ion-exchange reaction is commonly considered as a rather mild reaction to obtain metastable compounds. We also attempted to synthesize the lithium carbonophosphates directly by hydrothermal reaction. The attempts were not successful even under wildly varying synthesis conditions. This result also confirms the lack of thermodynamic stability of the lithium carbonophosphates predicted by the computations.

The formation temperature of the carbonophosphates with the first-period transition metals shows an interesting trend. The more one goes to the right in the periodic table, the higher the reaction temperature that is required to form a sidorenkite phase. A pure Mn phase can be formed at a temperature as low as 90 °C, similar to the Fe phase. The Co phase can also be formed at 90 °C, but requires a much longer reaction time than the Mn and Fe phases. For the Ni phase, no sidorenkite phase is formed at 140 °C even after 3 days. At 160 and 180 °C, after 20 h, the Ni sidorenkite phase can be formed but with unidentified amorphous impurities. Only at temperature above 200 °C and after 20 h can single-phase Ni sidorenkite sample be obtained. For Cu, even higher temperature is required: at >220 °C, Cu sidorenkite can be obtained but with the presence of minor unidentified impurities. Such a trend of increasing formation temperature agrees well with our computational results. As summarized in Table 1, with the increase of atomic number, the absolute value of the computed *energy below the hull* becomes smaller, indicating less driving forces to move the equilibrium from the competing phases to the sidorenkite phase side. Thus, the less energetically stable, the higher temperature and/or longer reaction time are required to form the sidorenkite phase. The only exception to this trend is Ni, which is computed to be very stable but requires a high temperature to form. This may be explained by the fact that Ni forms a relatively stable intermediate phase (which has not been identified yet) that decomposes only at higher temperatures. This trend may also be part of the reason that the Zn phase was not synthesized. The formation temperature of the Zn phase may be higher than 240 °C, beyond the temperature limit of our hydrothermal reactor.

The unit cell size of the carbonophosphates is obviously influenced by the size of the metal in the M site. Figure 8 shows the cell parameters of the carbonophosphates of the first-period 2+ transition metals and their Shannon ionic radii with octahedral coordination. It can be seen that the cell parameters and the volume of the unit cell are positively correlated with the size of the transition metal. Even with the Sr compound being a outlier, it seems that 2+ cations with radius 0.69−0.83 Å are most favored to form sidorenkite structure. The sidorenkite structure is flexible and can form with many different 2+ ion chemistries, We already demonstrated that a solid solution of Mn−Fe and Co−Mn can be formed in this structure, and it is therefore likely that many solid solutions of the type $Na_3(M1_xM2_{1-x})(PO_4)(CO_3)$ could be synthesized.

Finally, the successful chemical de-sodiation with the sodium iron carbonophosphates demonstrates that these materials have the potential to function as Na intercalation electrodes. Only one Na per formula is extracted in the chemical de-sodiation, corresponding to an active Fe^{2+}/Fe^{3+} redox couple. The Fe^{3+}/Fe^{4+} redox couple is generally not active with polyanion cathode materials in Li-ion batteries. Therefore, the sodium iron carbonophosphate may not have high capacity (<100 mAh/g) as an electrode material. However, other transition metals, such as Mn and Co, may be active with both their 2+/3+ and 3+/4+ redox couples, which would provide high capacities over 190 mAh/g. The ability to form fully mixed solid solutions of different transition metals with the sidorenkite structure also provides a potentially effective approach to tune the size of the Na ion channels in the structure, therefore improving the Na ion diffusivity.

■ CONCLUSIONS

The carbonophosphates are a rarely studied yet potentially important class of compounds. We have successfully synthe-

dx.doi.org/10.1021/ja3040834 | J. Am. Chem. Soc. 2012, 134, 19619−19627

sized seven carbonophosphates with the general formula $Na_3M(PO_4)(CO_3)$ (M = Mg, Mn, Fe, Co, Ni, Cu, Sr). The synthesis of these compounds confirms that our previous computations accurately predict the stability of novel materials. We analyzed the formation condition of these compounds and related the failure to form other carbonophosphates to a lack of energetic driving force, which can be computationally identified. From these results, it is clear that computations can offer some guidance as to the synthesis of novel materials. Our preliminary work shows that the carbonophosphates can potentially be used as intercalation electrodes for Na-ion batteries.

■ ASSOCIATED CONTENT

Supporting Information

XRD pattern and Rietveld refinement plots of the Fe, Mn, Cu, and Mg samples; XRD pattern of the Sr sample and the Co–Mn solid solution sample; and Rietveld refinement result of the chemical de-sodiated iron carbonophosphate sample. This material is available free of charge via the Internet at http://pubs.acs.org.

■ AUTHOR INFORMATION

Corresponding Author

gceder@mit.edu

Present Address

[§]Institut de la matière condensée et des nanosciences (IMCN) Université Catholique de Louvain Chemin des étoiles 8, bte L7.03.01 1348 Louvain-la-Neuve Belgium.

Notes

The authors declare no competing financial interest.

■ ACKNOWLEDGMENTS

This work was supported by the Robert Bosch Company, by Umicore, and by the Assistant Secretary for Energy Efficiency and Renewable Energy, Office of Vehicle Technologies of the U.S. Department of Energy under Contract No. DE-AC02-05CH11231, under the Batteries for Advanced Transportation Technologies (BATT) Program through subcontract no. 6806960. Dr. Clare Grey, Dr. Olivera Zivkovic, and Dr. Linshu Du are acknowledged for helpful discussions. The authors also thank the General User Program of the National Synchrotron Light Source for awarding synchrotron beam time at beam lines X16C and X14A, and thank Dr. Peter Stephens and Dr. Jianming Bai for their help with synchrotron XRD data collection. H.C. thanks Dr. Scott Speakman for helpful discussions.

■ REFERENCES

(1) Hautier, G.; Jain, A.; Ong, S. P.; Kang, B.; Moore, C.; Doe, R.; Ceder, G. *Chem. Mater.* **2011**, *23*, 3945–3508.
(2) Jain, A.; Hautier, G.; Moore, C. J.; Ong, S. P.; Fischer, C. C.; Mueller, T.; Persson, K. A.; Ceder, G. *Comput. Mater. Sci.* **2011**, *50*, 2295–2310.
(3) Mueller, T.; Hautier, G.; Jain, A.; Ceder, G. *Chem. Mater.* **2011**, *23*, 3854–3862.
(4) Setyawan, W.; Gaume, R. M.; Lam, S.; Feigelson, R. S.; Curtarolo, S. *ACS Combinatorial Sci.* **2011**, *13*, 382–390.
(5) Madsen, G. K. H. *J. Am. Chem. Soc.* **2006**, *128*, 12140–12146.
(6) d'Avezac, M.; Luo, J. W.; Chanier, T.; Zunger, A. *Phys. Rev. Lett.* **2012**, *108*, 5.
(7) Hautier, G.; Fischer, C. C.; Jain, A.; Mueller, T.; Ceder, G. *Chem. Mater.* **2010**, *22*, 3762–3767.
(8) Kolmogorov, A.; Shah, S.; Margine, E.; Bialon, A.; Hammerschmidt, T.; Drautz, R. *Phys. Rev. Lett.* **2010**, *105*, 1–4.
(9) Hautier, G.; Jain, A.; Chen, H.; Moore, C.; Ong, S. P.; Ceder, G. *J. Mater. Chem.* **2011**, *21*, 17147–17153.
(10) Ma, X. H.; Chen, H. L.; Ceder, G. *J. Electrochem. Soc.* **2011**, *158*, A1307–A1312.
(11) Ong, S. P.; Chevrier, V. L.; Hautier, G.; Jain, A.; Moore, C.; Kim, S.; Ma, X. H.; Ceder, G. *Energy Environ. Sci.* **2011**, *4*, 3680–3688.
(12) Palomares, V.; Serras, P.; Villaluenga, I.; Hueso, K. B.; Carretero-Gonzalez, J.; Rojo, T. *Energy Environ. Sci.* **2011**, *5*, 5884–5901.
(13) Sauvage, F.; Laffont, L.; Tarascon, J. M.; Baudrin, E. *Inorg. Chem.* **2007**, *46*, 3289–3294.
(14) Xia, X.; Dahn, J. R. *Electrochem. Solid State Lett.* **2012**, *15*, A1–A4.
(15) Kresse, G.; Furthmuller, J. *Comput. Mater. Sci.* **1996**, *6*, 15–50.
(16) Perdew, J.; Burke, K.; Ernzerhof, M. *Phys. Rev. Lett.* **1996**, *77*, 3865–3868.
(17) Dudarev, S. L.; Savrasov, S. Y.; Humphreys, C. J.; Sutton, A. P. *Phys. Rev. B* **1998**, *57*, 1505–1509.
(18) (a) *Inorganic Crystal Structure Database*; Fachinformationszentrum Karlsruhe: Karlsruhe, Germany, 2006; http://www.fiz-karlsruhe.de/icsd.html. (b) *Powder Diffraction Files*; International Centre for Diffraction Data: Newtown Square, PA, 2012; http://www.icdd.com/products/.
(19) Wang, L.; Maxisch, T.; Ceder, G. *Phys. Rev. B* **2006**, *73*, 1–6.
(20) Chase, M. W. *NIST-JANAF Thermochemical Tables*; American Institute of Physics: Woodbury, NY, 1998.
(21) Khomyakov, A. *Int. Geol. Rev.* **1980**, *22*, 811–814.
(22) Lu, Z. G.; Chen, H. L.; Robert, R.; Zhu, B. Y. X.; Deng, J. Q.; Wu, L. J.; Chung, C. Y.; Grey, C. P. *Chem. Mater.* **2011**, *23*, 2848–2859.
(23) Lv, S.; Li, P.; Sheng, H.; Sun, W. D. *Mater. Lett.* **2007**, *61*, 4250–4254.
(24) Ellis, B. L.; Makahnouk, W. R. M.; Rowan-Weetaluktuk, W. N.; Ryan, D. H.; Nazar, L. F. *Chem. Mater.* **2011**, *22*, 1059–1070.
(25) Matts, I.; Chen, H. L.; Hautier, G.; Ceder, G. *ECS Meeting Abstr.* **2012**, *MA02*, 681.
(26) Chen, H. L.; Hautier, G.; Jain, A.; Moore, C.; Kang, B.; Doe, R.; Wu, L. J.; Zhu, Y. M.; Tang, Y. Z.; Ceder, G. *Chem. Mater.* **2012**, *24*, 2009–2016.
(27) Hautier, G.; Ong, S. P.; Jain, A.; Moore, C. J.; Ceder, G. *Phys. Rev. B* **2012**, *85*, No. 155208.
(28) Persson, K. A.; Waldwick, B.; Lazic, P.; Ceder, G. *Phys. Rev. B* **2012**, *85*, No. 235438.
(29) Chen, H. L.; Hautier, G.; Jain, A.; Moore, C.; Doe, R. E.; Kang, B. W.; Wu, L. J.; Zhu, Y. M.; Tang, Y. Z.; Ceder, G. *Chem. Mater.* **2012**, *24*, 2009–2016.